UNIVERSIDADE DE SÃO PAULO

INSTITUTO DE FÍSICA
CAIXA POSTAL 20516
01498 - SÃO PAULO - SP
BRASIL

PUBLICAÇÕES

IFUSP/P-900

ALGEBRAIC SCATTERING THEORY APPLIED TO HEAVY ION REACTIONS

A. Lépine-Szily
Instituto de Física, Universidade de São Paulo

Invited-talk presented at "XIV Nuclear Physics Symposium"
Oaxtepec / Mexico - 7-10 January 1991

Fevereiro/1991

ALGEBRAIC SCATTERING THEORY APPLIED TO HEAVY ION REACTIONS

A. Lépine-Szily
Departamento de Física Nuclear - Instituto de Física
Universidade de São Paulo
C.P. 20516 - 01498-São Paulo-SP - Brasil

ABSTRACT

Experimental results on back-angle anomaly in the $^{12}C + ^{24}Mg$ system at E_{CM} = 25.2 MeV and orbiting phenomena in $^{16}O + ^{10,11}B$ systems at E_{CM} = 18.8 and 19.9 MeV are presented. Both results are fully explained by coupled-channels calculations in the AST framework, coupling 7 reactions channels in the former and 22 reaction channels in the latter case.

1. INTRODUCTION

The algebraic approach to nuclear reactions (AST) allows the simple solution of problems where many reaction channels are coupled together[1,2]. We applied this approach in two situations, where the coupling between reaction channels should be very important. These situations are the back-angle anomaly, present mainly in nα systems of the s-d shell, and the orbiting phenomena. In the following we will summarize some issues of the algebraic approach, present our experimental data both on back-angle anomaly and orbiting phenomena and show the results of AST calculations, which explain the main features of data.

2. ALGEBRAIC APPROACH TO THE SCATTERING PROBLEM

Iachello and collaborators[1,2] have shown recently that the concept of dynamic symmetry fixes the functional form of the S-matrix. S-matrices can be obtained directly from group theory, without the use of the Schrödinger equation. This can be illustrated with the example of the non-relativistic Coulomb scattering, where the symmetry group is the SO(3,1), and from properties of this symmetry group one can derive the expression for the S-matrix, as

$$S_\ell(k) = \frac{\Gamma(\ell + 1 + iv(k))}{\Gamma(\ell + 1 - iv(k))} \qquad (1)$$

where v is called algebraic Coulomb potential and is by definition

$$v(k) = \frac{\mu Z_1 Z_2 e^2}{\hbar^2 k} \qquad (2)$$

This result can be applied in the case of low-energy heavy-ion reactions, where the Coulomb potential is very important. It is assumed that the form of the S-matrix, derived from SO(3,1) algebra, is still valid in the presence of the nuclear potential, and

$$S_\ell(k) = \frac{\Gamma(\ell + 1 + iv(\ell,k))}{\Gamma(\ell + 1 - iv(\ell,k))} \qquad (3)$$

where $$v(\ell,k) = \frac{\mu Z_1 Z_2 e^2}{\hbar^2 k} + v_N(\ell,k) \qquad (4)$$

where $v_N(\ell,k)$ is the algebraic nuclear potential. We determined the ℓ-dependence of $v_N(\ell,k)$, which produces the same elastic scattering S-matrix in eq.3 as a Woods-Saxon optical potential produces using the Schrödinger equation. The exact $v_N(\ell,k)$, obtained by numerical inversion of eq.3, was fitted by the parametrization below[3]

$$v_N(\ell,k) = \frac{v_R(k) + iv_I(k)}{\left[1 + \exp\frac{\ell - \ell_0(k)}{\Delta(k)}\right]}\left[\frac{2\ell}{\ell_0} + 1\right]^{-\pi/2} \qquad (5)$$

where $\ell_0(k) = R_0 k = \frac{R_0}{\hbar}\sqrt{2\mu\left[E_{CM} + Q - V_{CB}\right]}$ is grazing angular momentum (6)

and $\Delta(k) = ka$ (7)

and R_0 and a are respectively the radius and diffuseness of the system. Thus, the algebraic counterpart of the Woods-Saxon optical potential, is a complex, ℓ-dependent potential, which is well described by the parametrization of eq.5.

The main advantage of this algebraic approach lays in the simplicity of its generalization to the many channels problem. In the case of n reaction channels, the algebraic potential becomes a symmetrical, complex $n \times n$ matrix and the solution of the problem reduces to the diagonalization of the potential matrix. So, instead of solving n coupled differential equations which is the problem in the Schrödinger picture, one has to solve n coupled algebraic equations.

The diagonal elements of v correspond to potentials producing elastic scattering in channels $i = 1,2,\ldots n$ and they are described by equations 4 and 5, where the grazing angular momenta take into account the Q-value of the channel i. The off-diagonal elements v_{ij} correspond to coupling potentials producing transitions between states

In fig. 2 we present our experimental elastic angular distribution of $^{24}Mg(^{12}C, ^{12}C)^{24}Mg$, together with the results of the AST using the above algebraic potential (eqs. (4) and (5)) (solid line) and of optical model calculations (dashed line). The parameters used in the AST approach are $V_R = 2.0$ $V_I = 5.0$, $\ell_0 = 14.5$ and $\Delta = 1.7$. The optical potential parameters are V = 10 MeV, $r_0 = 1.318$ fm, a = 0.618 fm, W = 23,4 MeV, $r_{0I} = 1.199$ fm and $a_I = 0.552$ fm. Both calculations reproduce well the forward angle region and undersestimate the backward cross section, a feature common to strongly absorbing potentials. The oscillations and back-angle rise could be reproduced by decreasing Δ or V_I, in analogy to the sharp edge or surface transparent optical potentials. However, our aim was not just reproducing the backward anomaly but getting a better understanding of the origin of these anomalies. We will see in the following that even with strongly absorbing potentials the inclusion of α-transfer couplings produces the backward rise in the elastic cross section.

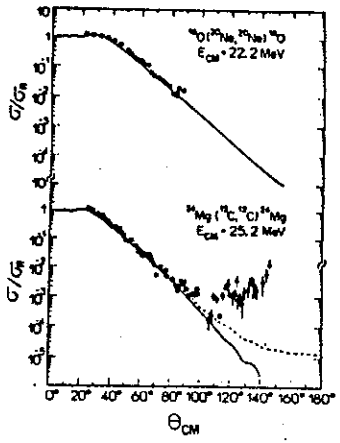

Fig.2 - Experimental elastic angular distribution of ^{12}C + ^{24}Mg measured in this work and of ^{16}O + ^{20}Ne (ref.[10]). The solid lines are AST calculations with the parameters presented in table 1. The dashed line is the optical model calculation, its parameters are quoted in the text.

The parameters that define the diagonal matrix elements of the outgoing channel ^{16}O + ^{20}Ne, were determined by fitting the experimental angular distribution [10] of ^{16}O + ^{20}Ne elastic scattering at E_{CM} = 22.2 MeV (see fig.2). The inelastic coupling strengths (Coulomb and nuclear) were calculated from experimental B(Eλ) and β_λ values using eq.(9) and the absolute normalization is obtained by fitting the 2^+ inelastic angular distribution. The hexadecapole deformations (β_4) of ^{24}Mg and ^{20}Ne were also included, producing direct coupling between the 0^+ and 4^+ states. The transfer coupling strengths were adjusted to fit the magnitude of the transfer cross sections.

The fits are in very good agreement with the data. The absolute magnitude, the period and phase of oscillations and the backward rise are well reproduced. The only cross section which is somewhat undersestimated by the calculations is that of the sum of the 4^+ and $2'^+$ states but the coupling to higher excited states, which was not taken into account, probably must be important.

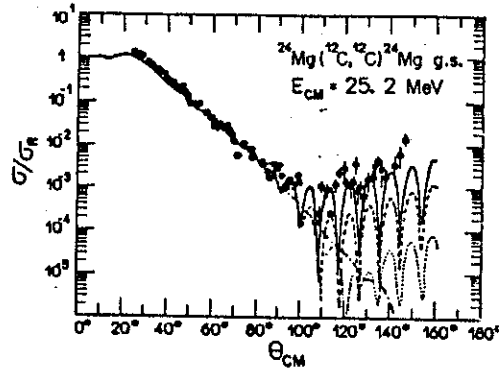

Fig.3 - Experimental elastic angular distribution of ^{12}C + ^{24}Mg. The dash-dotted line is the result of the AST calculation without any couplings, the dotted line with coupling between elastic and ground-state transfer channels, the dashed line with couplings to 0^+ and 2^+ transfer states, the solid line with couplings to 0^+, 2^+ and 4^+ transfer states.

In fig.3 we show the effect on the elastic angular distribution due to the coupling of transfer channels added one-by-one. We can verify that the backward increase in the elastic cross section comes from the coupling to the transfer states. The contribution of excited transfer states is very important. Similar calculations, coupling only with inelastic 2^+ and 4^+ states, have shown that the effect of the inelastic couplings is much weaker at back angles.

Concluding, we measured six fairly complete angular distributions of elastic, inelastic and α-transfer reactions of the ^{12}C + ^{24}Mg system at E_{CM} = 25.2 MeV. We used the AST to couple all the channels measured in our experiment. The inelastic coupling strengths were derived from available B(Eλ) and β_λ information and a good fit was obtained for all channels. The back-angle rise in the elastic cross section is fully explained by the coupling between elastic and transfer channels.

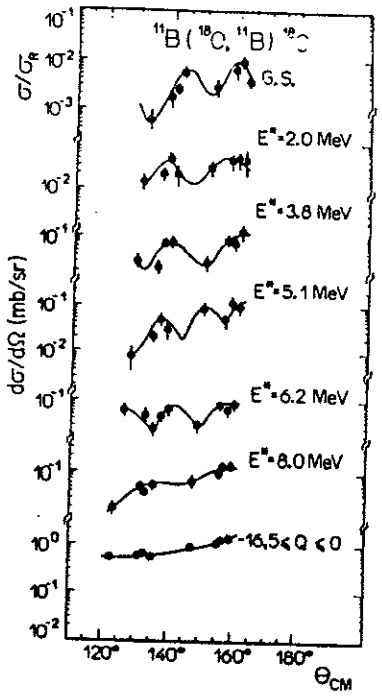

Fig. 5 - The angular distributions of individual peaks in inelastic boron spectra of $^{18}O + ^{11}B$ reaction. The solid line is a guide to the eye.

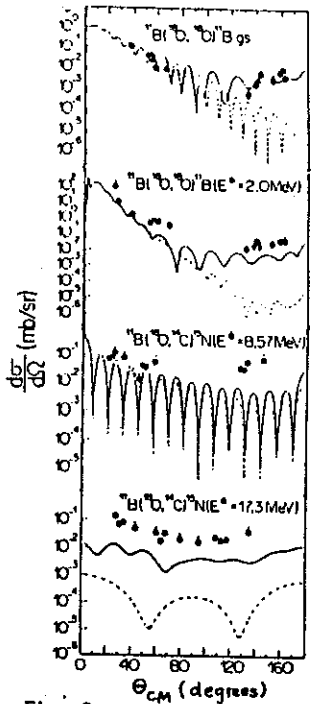

Fig. 6 - The dots are the experimental data of indicated reactions and the solid and dashed lines are respectively AST calculations with and without coupling to all other channels.

dependence. This can be verified for both $^{18}O + ^{10,11}B$ systems for Z = 5,6 and 7 on figure 7. The nitrogen and carbon cross sections are plotted on the same angular distribution, assuming arbitrarily that Z = 7 is emitted forward and Z = 6 backward. For the nitrogen angular distribution of the system $^{18}O + ^{10}B$, a deviation from $1/sin(\theta_{cm})$ behaviour is expected due to fusion contamination at forward angles. For the $^{18}O + ^{11}B$ system, the very forward angle nitrogen spectra are affected by a Z = 8 queue, which corresponds to reactions in the S1 detector due to intense counting rate of elastic scattering. This fact invalidates the estimation of the nitrogen emission cross section at forward angles. As nitrogen and carbon fragments are emitted by the same DNC, they have the same characteristic lifetime and should have similar angular distributions. The deviation from a $1/sin(\theta_{cm})$ pattern of the nitrogen angular distribution cannot be due to a shorter lifetime, as suggested recently [14], but only due to contamination of a different process, as long as we assume the fragments being provenient from the decay of an orbiting dinuclear complex.

The total Q-value and angle integrated cross sections for both studied systems are very similar, $\sigma(^{18}O + ^{10}B) = 9 \pm 1$mb, $\sigma(^{18}O + ^{11}B) = 9 \pm 1$mb, $\sigma(^{13}C + ^{15}N) = 19 \pm 2$mb and $\sigma(^{14}C + ^{16}N) = 21 \pm 2$mb, suggesting that the orbiting process is not affected by special nuclear structure effect, due to one neutron excess. For $^{18}O + ^{11}B$ we also detected the Z = 3 and 4 fragments, which present the same $1/sin(\theta_{cm})$ behaviour and have total cross sections of respectively 5 ± 1mb and 4.5 ± 1mb. In both systems $^{18}O + ^{10,11}B$, the total orbiting cross sections in the transfer channel (C + N) are higher than in the inelastic channel (O + B). This is easy to understand, since the ground state Q-values of both transfer reactions are very positive (Q_{gs} = +8.04 and +4.76 MeV respectively) and so the C + N systems have more excited states at the same Q-value.

The transition from strongly oscillating to smooth behaviour of the angular distribution of individual peaks suggested us the necessity for a more detailed description of the orbiting process.

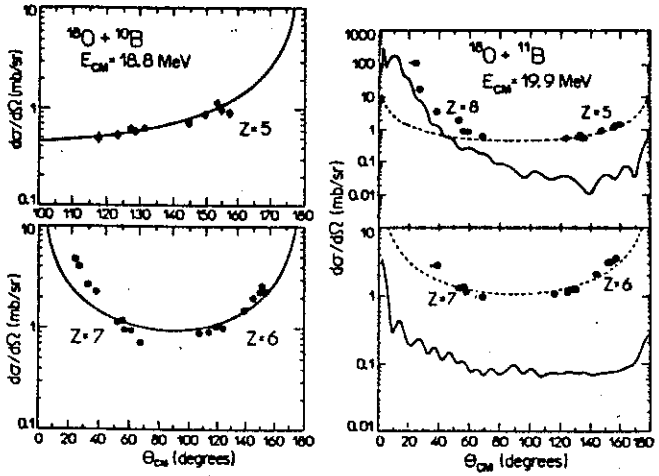

Fig. 7 - The Q-value integrated ($-18.MeV \leq Q \leq Q_{gs}$) experimental angular distributions for Z = 5,6 and 7 fragments for $^{18}O + ^{10,11}B$. The forward and backward data are obtained detecting the oxygen (sum of peaks of E*=2.MeV and E*=3.8MeV) or boron spectra and nitrogen or carbon spectra respectively. The curve through the experimental points is just the $1/sin\theta_{CM}$ function, normalized to the absolute cross-section. The solid curve in the case of $^{18}O + ^{11}B$ system is the result of AST calculation for the Q-value integrated inelastic and transfer cross-sections.

scheme necessary for obtaining the orbiting pattern is only possible to be calculated, at the moment, in AST frame. The algebraic approach reveals to be a powerful framework in nuclear reaction studies involving many channels.

The collaboration of J.M. Oliveira, P. Fachini, R. Lichtenthäler Fº, M.M. Obuti, W. Sciani, M.K. Steinmayer and A.C.C. Villari in the experimental measurements and in data reduction is acknowledged, as well as the financial support of CNPq.

REFERENCES

1. Y. Alhassid, F. Iachello and B. Shao. Phys.Lett., B201 (1988) 183.
2. Y. Alhassid, F. Iachello. Nucl.Phys., A501 (1989) 585 and references therein.
3. R. Lichtenthäler Fº, L.C. Gomes. To be published.
4. P. Braun-Munzinger and J. Barrette. Phys.Rep., 87 (1982) 209 and reference therein.
5. O. Portezan. Thesis, 1988 Universidade de São Paulo, to be published.
6. M.S. Hussein, A.N. Aleixo, L.F. Canto, P. Carrilho, R. Donangelo and L.S. de Paula. J.Phys., G 13 (1987) 967.
7. R. Lichtenthäler Fº, A. Lépine-Szily, A.C.C. Villari and O. Portezan Fº. Phys.Rev. C39 (1989), 884.
8. A. Lépine-Szily, R. Lichtenthäler Fº, M.M. Obuti, J.M.de Oliveira Jr., O. Portezan Fº, W. Sciani and A.C.C. Villari. Phys.Rev., C40 (1989), 681.
9. A. Lépine-Szily, M.M. Obuti, R. Lichtenthäler Fº, J.M.de Oliveira Jr. and A.C.C. Villari. Phys.Lett., B243 (1990), 23.
10. R. Stock, U. Jahnke, D.L. Hendrée, J. Mahoney, C.F. Maguire, W.F. Schneider, D.K. Scott and G. Wolschin. Phys.Rev., C14 (1976), 1824.
11. D. Shapira, J.L.C. Ford Jr., J. Gomez del Campo, R.G. Stokstad and R.M. DeVries. Phys.Rev.Lett., 43 (1979), 1781.
12. D. Shapira, R. Novotny, Y.D. Chan, K.A. Erb, J.L.C. Ford Jr., J.C. Peng and J.D. Moses. Phys.Lett., 114B (1982), 111.
13. B. Shivakumar, D. Shapira, P.H. Stelson, M. Becherman, B.A. Harmon, K. Teh and D.A. Bromley. Phys.Rev.Lett., 57 (1986), 1211 and references therein.
14. A. Szanto de Toledo, L. Fante Jr., R.M. Anjos, N. Added, M.M. Coimbra, M.C.S. Figueira, N. Carlin Fº, E.M. Szanto, M.S. Hussein and B.V. Carlson. Phys.Rev., 42C (1990), R815.